J. Phys. Chem. A **2006,** *110,* 6122−6128

Structures of Heterogeneous Proton-Bond Dimers with a High Dipole Moment Monomer: Covalent vs Electrostatic Interactions

Travis D. Fridgen[†]

Department of Chemistry, Memorial University of Newfoundland, St. John's, NL, Canada A1C 5S7

Received: December 15, 2005; In Final Form: March 16, 2006

A number of calculated structures of heterogeneous proton-bound dimers containing monomers such as acetonitrile, cyanamide, vinylene carbonate, and propiolactone, which have high dipole moments, are presented. These proton-bound dimers are predicted to have a structural anomaly pertaining to the bond distances between the central proton and the basic sites on each of the monomers. The monomers with the high dipole moments also have the larger proton affinity and, on the basis of difference in proton affinities, it would be expected that the proton would be closer to this monomer than the one with the lower proton affinity. However, the proton is found to lie substantially closer to the monomer with the lower proton affinity in most cases, unless the difference in proton affinity is too large. Simply stated, the difference in proton affinities is smaller than the difference in the affinity to form an ion−dipole complex for the two monomers and it is the larger affinity for the high dipole moment monomer (which also has the higher proton affinity) to form an ion−dipole complex that is responsible for the proton lying closer to the low proton affinity monomer. The bond distances between the central proton and the monomers are found to be related to the difference in proton affinity. It is found, though, that the proton-bound dimers can be grouped into two separate groups, one where the proton-bound dimer contains a high dipole moment monomer and one group where the proton-bound dimer does not contain a high dipole moment monomer. From these plots it has been determined that a high dipole moment monomer is one that has a dipole moment greater than 2.9 D.

1. Introduction

Protonated clusters are of particular interest to chemists due to the strong ionic hydrogen bonding that occurs. Proton-bound dimers can be thought of as the first stage of solvation of a protonated molecule. The early stages of the solvation process is not a clearly understood phenomenon but is of considerable interest.[1,2] The thermochemistry of protonated clusters has been widely studied and, more recently, the spectroscopy of homogeneous[3−9] and heterogeneous proton-bound dimers in the gas phase has been reported. Studies of protonated clusters, or ion−molecule complexes to some extent rely upon theoretically calculated properties, including structures to interpret the experimental results.

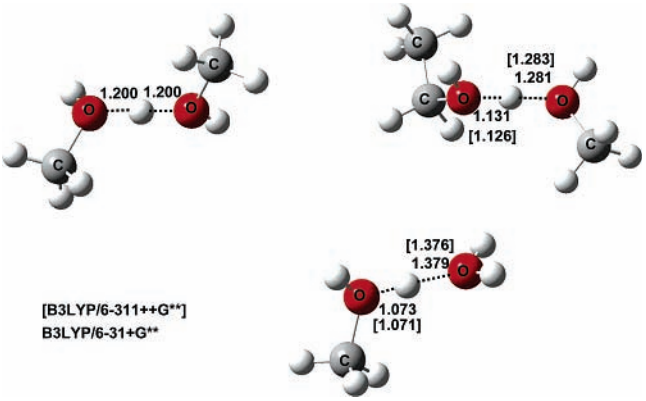

Figure 1. Geometries of some heterogeneous proton-bound dimers containing methanol and showing that the proton lies closer to the monomer with the higher proton affinity.

Typically, homogeneous proton-bound dimers are symmetric about the proton as shown for the B3LYP/6-31+G** calculated structure of the proton-bound methanol dimer in Figure 1. The water proton-bound dimer is predicted to be of C_2 symmetry at the highest computational levels,[10] and the proton-bound dimer of acetonitrile has D_{3d} symmetry.[11] For mixed proton-bound dimers, such as that of dimethyl ether and tetrahydrofuran, mixed alcohol proton-bound dimers,[12] and alcohol/ether proton-bound dimers,[13] the proton is predicted to lie closer to the monomer with the greater proton affinity, as might be expected. This is exemplified in Figure 1 for the methanol/ethanol and methanol/water proton-bound dimers. The binding energies of mixed proton-bound dimers has also been shown to be dependent upon the proton affinity difference[14] of the monomers for asymmetric oxygen *n*-donor bases,[15,16] nitrogen *n*-donor, and mixed nitrogen/oxygen *n*-donor bases as well as mixed dimers containing sulfur *n*-donor bases.[17] In a more recent paper it has even been shown that the wavenumber position of the O−H−O asymmetric stretching vibration of mixed proton-bound dimers may be correlated with the difference in proton affinities between the two monomers.

For some mixed proton-bound dimers the proton is predicted by theory to lie closer to the monomer with the lower proton-affinity. For example, MP2/6-31+G*,[18−20] MP2/6-311G**,[21] and B3LYP/cc-pVDZ calculations predict the proton to lie substantially closer to the methanol oxygen than the acetonitrile nitrogen for the proton-bound dimer of acetonitrile and methanol, even though the proton affinity of acetonitrile (779.2 kJ mol^{-1}) is larger by 24.9 kJ mol^{-1} than that of methanol (754.3 kJ mol^{-1}).[22] Similarly, the proton in the hydrogen cyanide/water

---

[†] Email: tfridgen@mun.ca.

10.1021/jp057335t CCC: $33.50

CHART 1

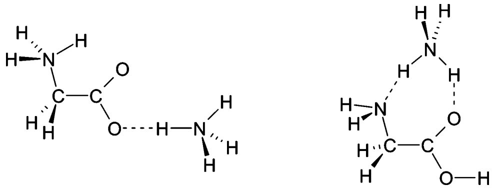

proton-bound dimer is predicted to lie closer to water, even though its proton affinity is 22 kJ mol^{-1} lower than that of hydrogen cyanide.[23] The most stable predicted structure of ammonia bound to protonated glycine resembles a complex between protonated ammonia and neutral glycine (or the zwitterionic form; see Chart 1), even though the proton affinity of glycine is some 30 kJ mol^{-1} higher than that of ammonia.[24]

The root of this structural anomaly has, to the author's knowledge, been given a cursory discussion only once previously with respect to the methanol/acetonitrile proton-bound dimer.[21] The position of the proton in the methanol/acetonitrile proton-bound dimer (as discussed above) was attributed to the ability of the proton-bound dimer to lower its overall dipole moment by shortening the O$-$H$^+$ bond and lengthening the H$^+$$-$N bond. The dipole moments of methanol and acetonitrile are 1.70 and 3.92 D, respectively. The dipole moment of the proton-bound dimer was found to be 1.60 D in the optimized structure. Lengthening and freezing the O$-$H$^+$ bond to 1.5 Å resulted in a shorter H$^+$$-$N, a 22 kJ mol^{-1} increase in energy and an increase in the dipole moment to 3.41 D. However, when the proton affinity difference is very large between the two monomers (i.e., in acetonitrile/water), the proton-bound dimer adopts the "normal" structure with a very high dipole moment. The purpose of this paper is to more fully explore the structures of heterogeneous proton-bound dimers. A number of predicted structures of proton-bound dimers where the proton is predicted to lie closer to the monomer with the lower proton affinity will be presented. A simple model based on the interplay between electrostatic and covalent bonding of the proton will be presented and tested on a few model systems namely the acetonitrile/methanol, water/methanol, and acetonitrile water proton-bound dimers. This model is presented, not as a predictive tool, but as an explanation as to why the proton lies closer to the monomer with the lower proton affinity in some heterogeneous proton-bound dimers with "high dipole moment monomers".

2. Computational Methods

The purpose of this paper is not to study the dependence of the structures of proton-bound dimers on the method of calculation or the basis set used. However, for some proton-bound dimers, structures were calculated at various levels of theory such as B3LYP/6-31+G**, B3LYP/6-311++G**, B3LYP/6-311++G(2df,2pd), MP2/6-311G** and QCISD/6-31+G** to ensure that the "anomaly" in the proton-bound dimers' structures are not simply due to the method of calculation. All structures presented were verified as minima on the potential energy surface by the absence of imaginary vibrational frequencies. All structures presented are also believed to be global minima as far as conformational changes are concerned. Where conformational isomers are possible, many attempts were made to find the lowest-energy structures. G3MP2 calculations were done to obtain proton affinities for vinylene carbonate and β-propiolactone, for which no experimental values exist. Dipole moments were also calculated using B3LYP and the 6-311++G(2df,2pd) basis set to compare to experimental values and use as an estimate where no experimental values exist. Calculations were done using the Gaussian '03 suite of programs.[25]

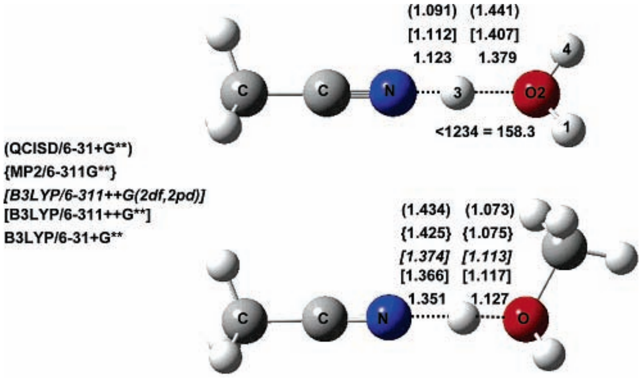

Figure 2. Geometries of acetonitrile/water and acetonitrile/proton-bound dimers.

3. Results and Discussion

In Figure 2 are presented the calculated structures for the acetonitrile/water and acetonitrile/methanol proton-bound dimers. The proton in the water/acetonitrile proton-bound dimer is significantly closer to acetonitrile than to water, as expected on the basis of the much higher proton affinity of acetonitrile, 779.2 vs 691 kJ mol^{-1}. The N$-$H bond is slightly longer, by about 0.11 Å than that predicted for protonated acetonitrile (1.011 Å) at the B3LYP/6-31+G** owing to some "sharing" of the binding proton. The structure of the proton-bound dimer resembles an electrostatically bound ion$-$dipole complex with protonated acetonitrile bound along the dipole moment of water.

As stated previously, the structure of the methanol/acetonitrile proton-bound dimer seems odd based solely on the proton affinity differences. Acetonitrile has a proton affinity that is 24.9 kJ mol^{-1} higher than that of methanol yet the H$^+$$-$O bond is significantly shorter than the H$^+$$-$N bond. The bond lengths predicted by a number of different levels of theory are shown in Figure 2 for comparison. It is obvious that at even very high levels of theory the result is quite similar, the proton is closer to methanol than to nitrogen. In Table 1, the geometry of three other acetonitrile-containing proton-bound dimers along with the proton affinity differences are tabulated. Note that except for the proton-bound dimers containing water and formaldehyde all of these proton-bound dimers have longer H$^+$$-$N than H$^+$$-$O bond distances despite acetonitrile having the larger proton affinity. For the acetonitrile/water and acetonitrile/formaldehyde proton-bound dimers, the proton affinity difference is very large.

It is interesting to note that the proton affinity differences between ethanol and methanol and between acetonitrile and methanol are about the same, 22.1 and 24.9 kJ mol^{-1}, respectively. In the ethanol/methanol proton-bound dimer (Figure 1), the proton is closer to ethanol (higher proton affinity), but as discussed above, the proton in the acetonitrile/methanol proton-bound dimer (Figure 2) is closer to methanol (lower proton affinity). The other difference with these proton-bound dimers is that acetonitrile has a very high dipole moment 3.92 D, which is thought to be the reason for the predicted structural anomaly. It was decided to explore other proton-bound dimers where one of the monomers has a high dipole moment.

In Figure 3 are shown some proton-bound dimers containing high dipole moment monomers that also have the higher proton affinity of the two monomers comprising the proton-bound dimer. The dipole moments and proton affinities of the monomers used in this study are listed in Table 2 along with

TABLE 1: Calculated[a] H^+−Monomer Bond Distances and Monomer Proton Affinity Differences[b] for Proton-Bound Dimers Containing High Dipole Moment Monomers

proton-bound dimer A/B	H^+- -A/Å	H^+- -B/Å	ΔPA/kJ mol^{-1} ($PA_A - PA_B$)
CH_3CN/H_2O	1.123	1.379	88.2
CH_3CN/CH_2O	1.166	1.318	66.3
CH_3CN/CH_3OH	1.351	1.127	24.9
CH_3CN/CH_3CHO	1.405	1.079	10.7
CH_3CN/CH_3CH_2OH	1.408	1.095	2.8
NH_2CN/H_2O	1.096	1.438	114.6
NH_2CN/CH_2O	1.131	1.375	92.7
NH_2CN/CH_3OH	1.285	1.172	51.3
NH_2CN/CH_3CHO	1.353	1.126	37.1
NH_2CN/CH_3CH_2OH	1.353	1.123	29.2
NH_2CN/CH_3CH_2CHO	1.384	1.106	19.6
NH_2CN/CH_3OCH_3	1.434	1.074	13.6
NH_2CN/CH_3COCH_3	1.462	1.069	−6.4
$C_3H_4O_3/H_2O$	1.058	1.424	123.2
$C_3H_4O_3/CH_2O$	1.071	1.400	101.3
$C_3H_4O_3/CH_3OH$	1.149	1.261	59.9
$C_3H_4O_3/CH_3CH_2OH$	1.257	1.152	37.8
$C_3H_4O_3/CH_3OCH_3$	1.346	1.089	22.2
$C_3H_4O_3/CH_3COCH_3$	1.389	1.073	2.2
$C_3H_4O_2/H_2O$	1.073	1.399	103.2[c]
$C_3H_4O_2/CH_2O$	1.092	1.367	81.3[c]
$C_3H_4O_2/CH_3OH$	1.242	1.169	39.9[c]
$C_3H_4O_2/CH_3CH_2OH$	1.322	1.110	17.8[c]
$C_3H_4O_2/CH_3OCH_3$	1.387	1.073	2.2[c]
$C_3H_4O_2/CH_3COCH_3$	1.423	1.064	−17.8
$C_3H_2O_3/H_2O$	1.075	1.382	93.6[c]
$C_3H_2O_3/CH_2O$	1.103	1.336	71.7[c]
$C_3H_2O_3/CH_3OH$	1.273	1.137	30.3[c]
$C_3H_2O_3/CH_3CH_2OH$	1.341	1.093	8.2[c]
$C_3H_2O_3/CH_3OCH_3$	1.396	1.063	−7.4
$C_3H_2O_3/CH_3COCH_3$	1.436	1.053	−27.4
HCN/H_2O	1.289	1.177	21.9
HCN/CH_2O	1.405	1.103	0.0
NH_2CH_2CN/CH_3COCH_3	1.060	1.492	12.9

[a] B3LYP/6-31+G**. [b] Taken from ref 22. [c] The proton affinities of propiolactone and vinylene carbonate were estimated using G3MP2 calculations.

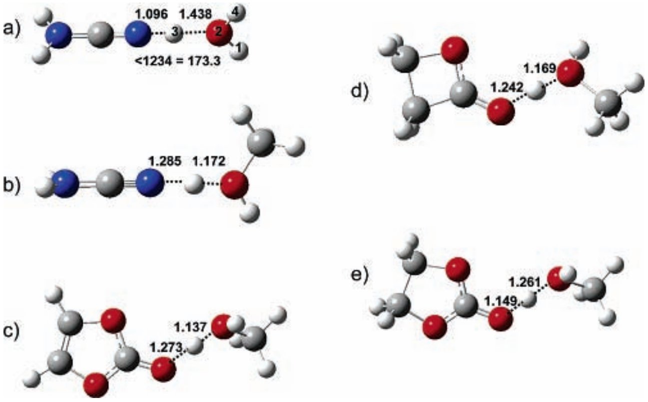

Figure 3. B3LYP/6-31+G** geometries of (a) cyanamide/water, (b) cyanamide/methanol, (c) vinylene carbonate/methanol, (d) β-propiolactone/methanol and (e) ethylene carbonate/methanol mixed proton-bound dimers. In all cases, the first monomer listed has the higher proton affinity (see Table 1 for proton affinity differences).

computed values. The proton affinities used to obtain proton affinity differences are all experimental values except for β-propiolactone and vinylene carbonate whose proton affinities were calculated using G3MP2 theory. Comparison of the computed and experimental proton affinities clearly suggests that the G3MP2 values for vinylene carbonate and β-propiolactone are dependable.

TABLE 2: Dipole Moments and Proton Affinities

monomer	proton affinity/ kj mol^{-1} exp[a]	G3MP2	dipole moment/ D exp[b]	calc[d]
NH_2CH_2CN (aminoacetonitrile)	824.9			4.61
$C_3H_4O_3$ (ethylene carbonate)	814.2	817.6	4.81[c]	5.51
$C_3H_2O_3$ (vinylene carbonate)		784.6	4.55	4.68
NH_2CN (cyanamide)	805.6		4.27	4.64
$C_3H_4O_2$ (β-propiolactone)		794.2	4.18	4.36
CH_3CN (acetonitrile)	779.2	782.6	3.92	4.06
HCN (hydrogen cyanide)	712.9	712.9	2.98	3.05
CH_3COCH_3 (acetone)	812	815.5	2.88	3.10
CH_3CHO	772.6	772.6	2.69	2.91
CH_3CH_2CHO	786.0		2.52	
CH_2O	712.9	713.5	2.33	2.42
H_2O	691	689.3	1.85	1.95
CH_3OH	754.3	755.2	1.70	1.73
CH_3CH_2OH	776.4	776.4	1.69	1.75
CH_3OCH_3	792	792	1.30	

[a] Reference 22 unless otherwise noted. [b] Reference 31 unless otherwise noted. [c] Reference 32. [d] B3LYP/6-311++G(2df,2pd).

The water/cyanamide proton-bound dimer (Figure 3a), with a very large difference in proton affinities, has the expected geometry with the H^+−N bond shorter than the H^+−O bond. Replacing water with methanol (Figure 3b), which has a proton affinity lower by 51.3 kJ mol^{-1} than cyanamide, results in a structure where the proton is significantly closer to the oxygen atom of methanol. Similar structures are predicted for the vinylene carbonate/methanol and b-propiolactone/methanol (Figures 3c,d, respectively) proton-bound dimers where the proton affinity of methanol is lower by 30.3 and 39.9 kJ mol^{-1}. For the ethylene carbonate/methanol proton-bound dimer where the proton affinity difference is significantly larger, 59.9 kJ mol^{-1}, the proton lies closer to the basic site on ethylene carbonate. In Table 1 are listed 33 heterogeneous proton-bound dimers that contain a monomer mentioned above with a high dipole moment. In Table 1, the heterogeneous proton-bound dimers are organized in groups where each group corresponds to one of the monomers with a high dipole moment. It is worth noting that in each group as the proton affinity difference decreases, the proton gets closer to the low-proton-affinity monomer. This is a trend that would be expected.

The proton-bound dimers listed in Table 1 and mentioned so far that contain water or formaldehyde have structures that would be expected on the basis of the proton affinity. However, when the monomer with the high-dipole moment is HCN (2.98 D), the HCN/water and HCN/formaldehyde proton-bound dimers display the same structural anomaly even though the proton affinity of water is less than that of HCN by 22 kJ mol^{-1} and both HCN and formaldehyde have the same proton affinity.

A proton-bound dimer that is symmetric about the proton, such as the water proton-bound dimer or the methanol proton-bound dimer (in Figure 1) is a nonclassical 3-center−4-electron bond. The two highest occupied molecular orbitals in these species are bonding with respect to the central $O-H^+-O$ moiety, as shown in Figure 4. In a mixed proton-bound dimer, such as the methanol/ethanol proton-bound dimer, two extremes of bonding that involve the central proton can be considered. The bond between the proton and ethanol is a covalent bond. Inspection of the molecular orbitals shows that there is no net covalent bond between the protonated ethanol and the methanol molecule. Protonated ethanol is bound to methanol via an electrostatic or ion−dipole interaction. Similarly, inspection of the molecular orbitals for the water/HCN or methanol/acetonitrile proton-bound dimers reveals that there is not a significant

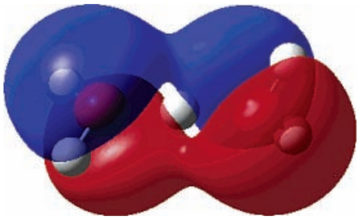

Figure 4. Highest occupied molecular orbital of the water proton-bound dimer which is exemplary of those for homogeneous proton bound dimers.

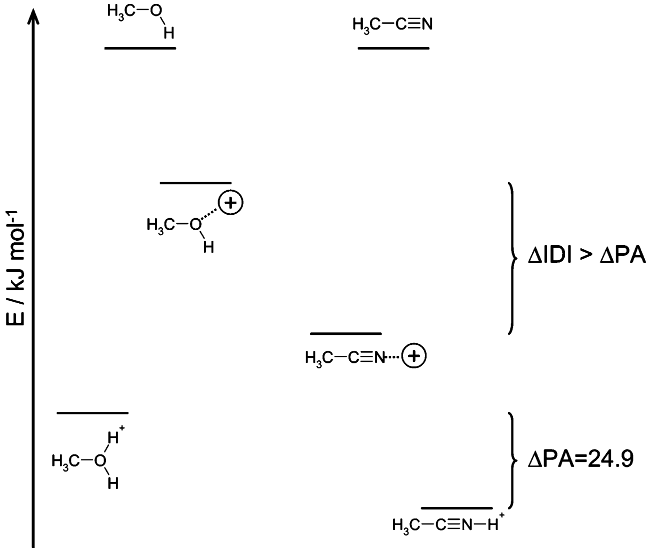

Figure 5. Schematic energy level diagram to explain the geometry of mixed proton-bound dimers containing a high dipole moment monomer in terms of the stabilization of the monomers by protonation and electrostatic charge solvation.

net covalent interaction between N and the proton, but there is a significant degree of covalent bonding between the proton and oxygen in both cases. The interaction between protonated methanol and acetonitrile (and between protonated water and HCN) is mostly electrostatic. For a proton-bound dimer such as that composed of methanol and ethanol, the bonding makes sense because ethanol has a larger proton affinity than methanol; thus the proton is covalently bound to ethanol and the methanol/protonated ethanol interaction is an electrostatic ion−dipole interaction. For the acetonitrile/methanol proton-bound dimer, thinking of the bonding in terms of a balance between electrostatic and covalent bonding might also explain why the proton is covalently bound to methanol even though the proton affinity is lower than that of acetonitrile by some 25 kJ mol^{-1}. What this means is that the sum of the covalent bond between the proton and methanol and an electrostatic interaction between the resulting ion and acetonitrile is lower in energy than the sum of the proton-acetonitrile covalent bond and electrostatic interaction between protonated acetonitrile and methanol. The difference between the electrostatic or ion−dipole interactions (ΔIDI) of methanol and acetonitrile is greater than the difference in proton affinities (ΔPA) for methanol and acetonitrile. This is shown schematically in Figure 5.

This explanation leads to a simple model which can be tested by electronic structure calculations. The model, very simply, is based on the balance between an electrostatic, or ion−dipole interaction, and a covalent interaction. In Figure 6a) are the results of three potential energy scans for the methanol/acetonitrile proton-bound dimer which will be discussed now. The black trace is a potential energy scan along the H$^+$−N bond

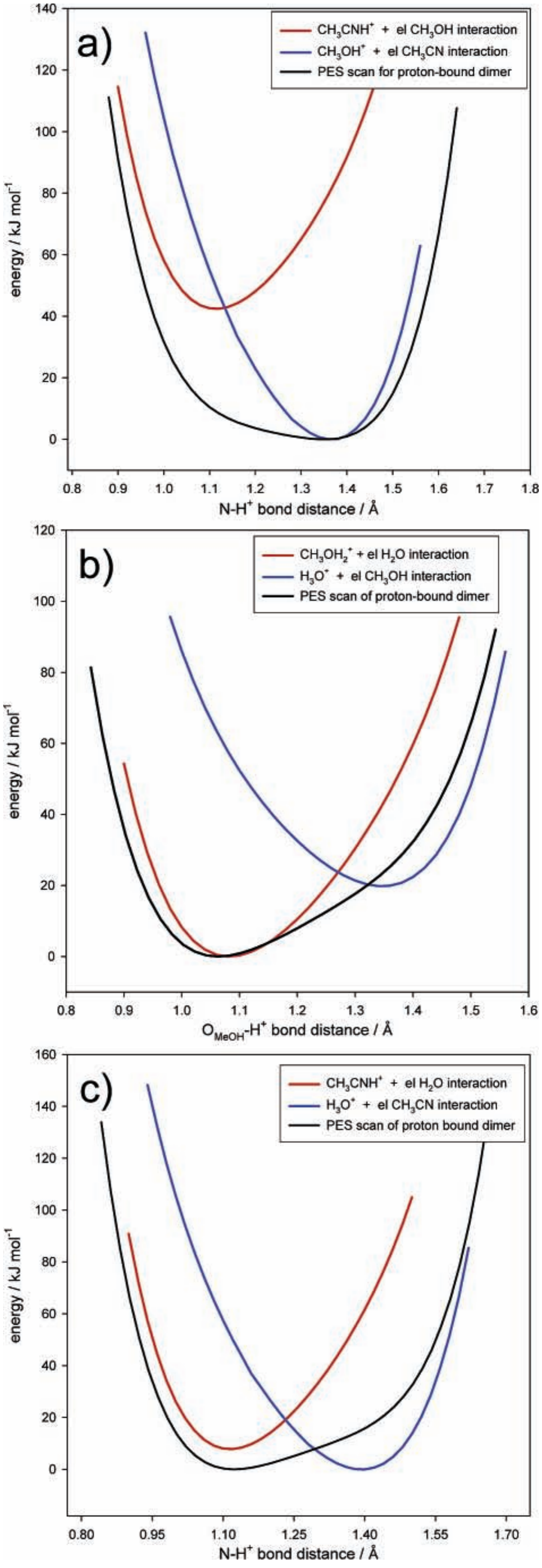

Figure 6. Relaxed potential energy diagram and potential energy diagrams from model calculations (see text for details) for (a) the acetonitrile/methanol proton-bound dimer, (b) the methanol/water proton-bound dimer, and (c) the acetonitrile/water proton-bound dimer.

distance. For consistency with the other scans, the O- -N bond length was held fixed at the value predicted in the optimized structure of the proton-bound dimer, the rest of the parameters were relaxed in that they were allowed to optimize. This trace shows the very broad, shallow potential for this particular proton-bound dimer, but that the minimum-energy structure is when the proton is farther from the nitrogen atom of acetonitrile and close to the oxygen atom of methanol. The blue trace in Figure 6a is composed of two potential energy scans. First a potential energy scan of protonated methanol was done by varying the H^+-O distance, freezing it, and optimizing the structure. Then, a scan was completed by putting a point charge along the dipole moment of acetonitrile and varying the point charge to N bond distance, mimicking a purely electrostatic interaction along the dipole of acetonitrile. Finally, the blue trace is the combination of these two potentials summed by putting the point charge and the proton at the same point. The zero energy of this curve is taken as the minimum point in energy. The red curve is the sum of a scan made by varying the H^+-N distance and one made by varying the point charge−oxygen distance, similar to that for the blue curve. The energy scales for the blue and red curves are the same.

What becomes apparent is that this simple model puts the minimum of energy in roughly the same place as the scan of the full molecule (black trace). The red curve, however, seems too high in energy using this simple model. There are many possible reasons for this. The modeled electrostatic interaction could either be too strong for acetonitrile or too weak for methanol. That it looks like the latter is correct, is only because the zero in energy was chosen to be for the blue curve. Another very likely reason could be the complete neglect of covalent interaction between the ion (protonated acetonitrile or protonated methanol) and the neutral in the red and blue curves.

In Figure 6b is a set of potential energy scans for the methanol/water proton-bound dimer similar to Figure 6a. For this system the model seems to reproduce the results of the scan of the full proton-bound dimer (black trace) much better than for the methanol/acetonitrile proton-bound dimer. The minimum in energy is adequately reproduced and the shape of the potential energy surface is also mimicked by the electrostatic/covalent model.

In Figure 6c is a similar set of potential energy scans as described above for the acetonitrile/water proton-bound dimer. This system is an example where the higher proton affinity of acetonitrile is not overcome by adopting a structure where protonated water is electrostatically bound to acetonitrile. The shape of the potential energy surface is, perhaps, reproduced by the electrostatic/covalent model. However, the model predicts that the H_3O^+/CH_3CN structure is slightly lower in energy than the H_2O/CH_3CNH^+ structure. This is opposite to what is predicted by calculations that optimize the full structure of the proton-bound dimer. As for the acetonitrile/methanol dimer, this simple model seems to either overestimate the stability associated with an ion−dipole complex of acetonitrile or underestimate the ion−dipole complex of water. The omission of covalent bonding between the ion and neutral also cannot be ruled out as a source of error in the model. It should be noted that calculations with larger basis sets and different levels (MP2) of theory had very little effect on the outcome of the model for the acetonitrile/methanol proton-bound dimer.

It is clear that the simple model presented might be too simple to be useful to predict the structure of a particular proton-bound dimer. In fact, producing the blue and red curves in Figure 6 requires significantly more effort than doing a simple geometry optimization on the proton-bound dimer. This model is not presented here for its predictive powers but to try to help explain why the heterogeneous proton-bound dimers containing a monomer with a high dipole moment are predicted to have the anomalous structures presented above. The answer to this seems to be a competition between ion−dipole interactions with and covalent bonding of the proton to the high dipole-moment monomer.

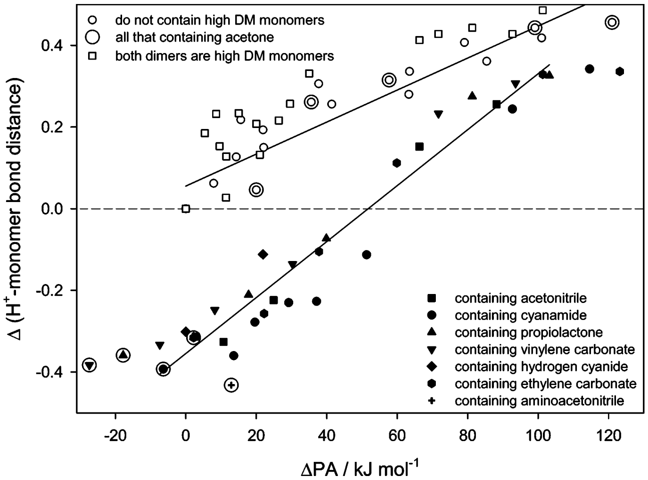

Figure 7. Plot of difference in H^+-monomer bond distance (lower proton affinity monomer$-H^+$ distance minus higher proton affinity monomer$-H^+$ distance; see text for details) vs the difference in proton affinity for the proton-bound dimers listed in Tables 1, 3 and 4.

In Figure 7 the difference in H^+-monomer bond distance is plotted versus the difference in proton affinity, ΔPA, for all the proton-bound dimers listed in Tables 1, 3 and 4. The difference in proton affinity is taken as the proton affinity of the monomer with the highest proton affinity minus that of the monomer with the lowest proton affinity so that $\Delta PA \geq 0$ kJ mol^{-1}. The difference in H^+-monomer bond distance is the H^+-B distance minus the H^+-A distance (see Table 1, 3 and 4). All values used to produce this plot are summarized in Tables 1, 3 and 4. The first thing to note is that there seem to be two groups of proton-bound dimers. The first group (filled-in symbols) is composed of proton-bound dimers containing only one high dipole moment (high-μ_D) monomer (data from Table 1). The second grouping is composed of two types of proton-bound dimers. The first (open circles, data from Table 3) are proton-bound dimers that do not have a high-μ_D monomer and the second (open squares, data from Table 4) contain proton-bound dimers in which both monomers are high-μ_D monomers. For the proton-bound dimers with one high-μ_D moment monomer, the linear regression suggests that when the difference in proton affinity is below ~52 kJ mol^{-1} in favor of the high-μ_D monomer, the proton lies closer to the monomer with the lower proton affinity. When the proton affinity difference is larger than this, the stabilization gained by forming a stronger ion−dipole complex is outweighed by the stronger covalent bond formed between the proton and the high-μ_D monomer. Note that this linear regression does not contain the two lowest and two highest differences in proton affinities as the difference in bond lengths seems to be converging below a proton affinity difference of about −5 and above about 100 kJ mol^{-1}.

For the proton-bound dimers without a high-μ_D monomer and those where both monomers are high-μ_D monomers the difference in H^+-monomer distance never becomes negative because when ΔPA is 0 kJ mol^{-1} the proton-bound dimers are symmetric. It is interesting that when both monomers in the proton-bound dimer are high-μ_D monomers, they display a trend similar

TABLE 3: Calculated[a] H^+−Monomer Bond Distances and Monomer Proton Affinity Differences[b] for Proton-Bound Dimers That Do Not Contain High Dipole Moment Monomers

proton-bound dimer A/B	H^+- -A/Å	H^+- -B/Å	ΔPA/kJ mol^{-1}
CH_3COCH_3/H_2O	1.038	1.494	121.0
CH_3OCH_3/H_2O	1.040	1.458	101.0
CH_3COCH_3/CH_2O	1.042	1.485	99.1
CH_3CH_2OH/H_2O	1.057	1.418	85.4
CH_3OCH_3/H_2CO	1.048	1.455	79.1
CH_3CH_2OH/H_2CO	1.070	1.406	63.5
CH_3OH/H_2O	1.080	1.360	63.3
CH_3COCH_3/CH_3OH	1.077	1.392	57.7
CH_3OH/H_2CO	1.096	1.352	41.4
CH_3OCH_3/CH_3OH	1.073	1.379	37.7
CH_3COCH_3/CH_3CH_2OH	1.093	1.354	35.6
CH_3CH_2OH/CH_3OH	1.131	1.281	22.1
H_2CO/H_2O	1.120	1.313	21.9
CH_3COCH_3/CH_3OCH_3	1.182	1.228	20.0
CH_3OCH_3/CH_3CH_2OH	1.104	1.322	15.6
CH_3CHO/CH_3OH	1.146	1.273	14.3
CH_3CH_2OH/CH_3CHO	1.175	1.237	7.9
H_2O/H_2O	1.199	1.199	0
CH_3OH/CH_3OH	1.200	1.200	0
CH_3CH_2OH/CH_3CH_2OH	1.201	1.201	0
CH_3OCH_3/CH_3OCH_3	1.199	1.199	0

[a] B3LYP/6-31+G**. [b] Taken from ref 22.

TABLE 4: Calculated[a] H^+−Monomer Bond Distances and Monomer Proton Affinity Differences[b] for Proton-Bound Dimers in Which Both Monomers Are High Dipole Moment Monomers

proton-bound dimer A/B	H^+- -A/Å	H^+- -B/Å	ΔPA[c]/kJ mol^{-1}
$C_3H_4O_3/HCN$	1.044	1.530	101.3
NH_2CN/HCN	1.093	1.521	92.7
$C_3H_4O_2/HCN$	1.059	1.502	81.3
$C_3H_2O_3/HCN$	1.059	1.487	71.7
CH_3CN/HCN	1.103	1.516	66.3
$C_3H_4O_3/CH_3CN$	1.088	1.419	35.0
NH_2CN/CH_3CN	1.162	1.378	26.4
$C_3H_4O_2/CH_3CN$	1.126	1.360	15.0
$C_3H_2O_3/CH_3CN$	1.142	1.327	5.4
CH_3CN/CH_3CN	1.262	1.262	0.0
$C_3H_4O_3/C_3H_2O_3$	1.090	1.347	29.6
$NH_2CN/C_3H_2O_3$	1.167	1.299	21.0
$C_3H_4O_2/C_3H_2O_3$	1.133	1.286	9.6
$C_3H_4O_3/C_3H_4O_2$	1.112	1.320	20.0
$NH_2CN/C_3H_4O_2$	1.217	1.244	11.4
$C_3H_4O_3/NH_2CN$	1.122	1.354	8.6

[a] B3LYP/6-31+G**. [b] Taken from ref 22. [c] The proton affinities of propiolactone and vinylene carbonate were estimated using G3MP2 calculations.

to those where neither of the monomers is a high-μ_D monomer. This can be explained because there is no greater stabilization gained by forming a strong ion−dipole complex with the monomer with the higher μ_D.

In the preceding discussion and in Figure 7, the structure in each of the two groups of proton-bound dimers seems only dependent upon the difference in proton affinity. In fact, there are very likely many other contributions, such as the difference in dipole moment and stearic factors. It is possible to, and attempts were made to try to, include a correlation with the difference in dipole moments between the two monomers; however, a correlation does not exist, at least on a global scale such as that by the proton affinity difference in Figure 7. What remains to be defined is what constitutes a "high-μ_D monomer". It might be expected that the structure of the proton-bound dimers be somewhat dependent on the dipole moment. This may be true; however, that is not apparent from these calculations. More than a smooth trend, there seems to be a cutoff for a monomer to be considered a high-μ_D monomer. Of the proton-bound dimers with high dipole moment monomers, the monomer with the lowest dipole moment is HCN with a dipole moment of 2.98 D. Of the other proton-bound dimers, that with the highest dipole moment mentioned so far is acetone with a dipole moment of 2.89. All proton-bound dimers containing acetone are indicated in Figure 7 by a large open circle around the symbol. When the proton-bound dimer is composed of acetone and a monomer with a greater dipole moment, it falls into the group with the closed symbols, one high-μ_D monomer. When the proton-bound dimer is composed of acetone and a monomer with a lower dipole moment, it falls into the group with closed circles, either no or both high-μ_D monomers. It is fairly clear that acetone, then is not a high-μ_D monomer. On the basis of these calculations, when a monomer has a dipole moment greater than somewhere between 2.89 and 2.98 D, it can be considered a "high-μ_D monomer". It is interesting to note that dipole-bound anions are predicted to be formed from molecules whose dipole moment is greater than 2.4 D.[26] The existence of dipole-bound anions have been confirmed for species with dipole moments down to 2.5 D[27] as well as for those with very large dipole moments[28] such as amino acids whose zwitterionic forms have been stabilized by solvation with a small number of water molecules.[29] This "minimum" in dipole moment to form dipole-bound anions is more or less in agreement with the definition of a "high-μ_D monomer", as determined by the present calculations.

It should be possible to detect this structural anomaly by measuring infrared spectra of these heterogeneous proton-bound dimers. For example, the C−O stretch of neutral methanol is observed[30] at 1033.5 cm^{-1} and predicted (B3LYP/6-31+G**, unscaled) to occur at 1045 cm^{-1}. The C−O stretch of protonated methanol is predicted to occur at a wavenumber value much lower, 798 cm^{-1}, due to the decreased C−O bond strength upon protonation of methanol. The proton-bound dimer of methanol shows an absorption at 982 cm^{-1} whereas the predicted position is 969 and 991 cm^{-1} for two different conformers of the proton-bound dimer, considerably red-shifted from the neutral position and blue-shifted from the position for protonated methanol because the C−O bond strength is only slightly weakened (and consequently elongated). For the cyanamide/methanol, propiolactone/methanol, vinylene carbonate/methanol and acetonitrile/methanol proton-bound dimers, the C−O stretching vibration is predicted to occur between 926 and 968 cm^{-1}, in all cases lower than that for the homogeneous methanol proton-bound dimer. This is due to these heterogeneous proton-bound dimers more resembling protonated methanol solvated by the high-μ_D monomer.

4. Conclusions

A model has been proposed to explain the predicted anomaly that exists for the structures of heterogeneous proton-bound dimers containing one monomer with a high dipole moment. The predicted bond length for the central proton to the basic site of the monomer with the higher proton affinity (and high dipole moment) is longer than that for the central proton to the basic site of the monomer with the lower proton affinity. The proton-bound dimer adopts a structure resembling a protonated molecule electrostatically bound to the monomer with the higher dipole moment. Forming a covalent bond between the proton and the monomer with the lower proton affinity and a strong electrostatic complex between the resultant protonated species with the high-μ_D monomer is lower in energy compared to forming a stronger covalent bond between the proton and the monomer with the higher proton affinity (and high dipole moment) and a weaker electrostatic complex between the resultant cation and the monomer with a small dipole moment. That is, the difference in proton affinities is smaller than the difference in the affinity to form an ion−dipole complex for the two monomers.

A plot relating the difference in H^+−monomer bond length with the difference in proton affinity reveals at least two groups of proton-bound dimers. One group contains proton-bound dimers where only one of the monomers contains a high-μ_D monomer and the other set contains proton-bound dimers without a high-μ_D monomer or with two high-μ_D monomers. Inspection of the dipole moments of the monomers making up the proton-bound dimers in the two groups reveals that a high dipole moment monomer is one that has a dipole moment greater than about 2.9 D based on these geometry calculations at the B3LYP/6-31+G** level of theory.

Acknowledgment. The Atlantic Computational Excellence Network (ACENet) and the Memorial University of Newfoundland Advanced Computation and Visualization Centre is gratefully acknowledged for free computational resources.

References and Notes

(1) (a) Lemoff, A. S.; Bush, M. F.; Wu. C. C.; Williams, E. R. *J. Am. Chem. Soc.* **2005**, *127*, 10276. (b) Lemoff, A. S.; Bush, M. F.; Williams, E. R. *J. Am. Chem. Soc.* **2003**, *125*, 13576 (and references therein).

(2) Xu, S.-J.; Nilles, J. M.; Bowen, K. H. *J. Phys. Chem.* **2003**, *119*, 10696 (and references therein)

(3) Fridgen, T. D.; MacAleese, L; Maitre, P.; McMahon, T. B.; Boissel, P.; Lemaire, J. *Phys. Chem. Chem. Phys.* **2005**, *7*, 2747.

(4) Fridgen, T. D.; McMahon, T. B.; MacAleese, L.; Lemaire, J.; Maitre, P. *J. Phys. Chem. A* **2004**, *108*, 9008.

(5) Moore, D. T.; Oomens, J.; van der Meer, A. F. G.; von Helden, G.; Meijer, G.; Valle, J.; Marshall, A. G.; Eyler, J. R. *ChemPhysChem* **2004**, *5*, 740.

(6) Asmis, K. R.; Pivonka, N. L.; Santambrogio, G.; Brummer, M.; Kaposta, C.; Neumark, D. M.; Woste, L. *Science* **2003**, *299*, 1375.

(7) Soca, N.; Dopfer, O. *J. Am. Chem. Soc.* **2004**, *126*, 9520.

(8) Hedrick, J. M.; Bopp, J. C.; Johnson, M. A. *J. Chem. Phys.* **2004**, *121*, 11523.

(9) Fridgen, T. D.; MacAleese, L; McMahon, T. B.; Lemaire, J.; Maitre, P. *Phys. Chem. Chem. Phys.* **2006**, *8*, 955.

(10) Valeev, E. F.; Schaefer, H. F., III. *J. Chem. Phys.* **1998**, *108*, 7197.

(11) Martin, J. M. L.; Aviyente, V.; Lifshitz, C. *J. Phys. Chem. A* **1997**, *101*, 2597.

(12) Fridgen, T. D.; McMahon, T. B. *J. Phys. Chem. A* **2003**, *107*, 668.

(13) Fridgen, T. D.; McMahon, T. B. *J. Phys. Chem. A* **2002**, *106*, 1576.

(14) Bain, L. *J. Phys. Chem. A.* **2003**, *107*, 11517. In this article the binding energy is correlated-to-a ratio of the proton affinities.

(15) Larson, J. W.; McMahon, T. B. *J. Am. Chem. Soc.* **1982**, *104*, 6255.

(16) Meot-Ner, M. *J. Am. Chem. Soc.* **1984**, *106*, 1257.

(17) Speller, C. V.; Meot-Ner, M. *J. Phys. Chem.* **1985**, *89*, 5217.

(18) Mayer, P. M. *J. Phys. Chem. A* **1999**, *103*, 3687.

(19) Mayer, P. M. *J. Phys. Chem. A* **1999**, *103*, 5905.

(20) Grabowy, J. A. D.; Mayer, *J. Phys. Chem. A* **2004**, *108*, 9726.

(21) Fridgen, T. D.; Keller, J. D.; McMahon, T. B. *J. Phys. Chem. A* **2001**, *105*, 3816.

(22) Lias, S. G.; Bartmess, J. E.; Liebman, J. F.; Holmes, J. L.; Levin, R. D.; Mallard, W. G. Ion Energetics Data. In *NIST Chemistry WebBook, NIST Standard Reference Database Number 69*; Linstrom, P. J., Mallard, W. G., Eds.; National Institute of Standards and Technology, Gaithersburg MD, 20899 (http://webbook.nist.gov), June 2005.

(23) Mayer, P. M. *J. Chem. Phys.* **1999**, *110*, 7779.

(24) Bulent, B.; Basma, M.; Aviyente, V.; Zhu, C.; Lifshitz, C. *Int. J. Mass Spectrom.* **2000**, *201*, 69.

(25) Frisch, M. J.; Trucks, G. W.; Schlegel, H. B.; Scuseria, G. E.; Robb, M. A.; Cheeseman, J. R.; Montgomery, J. A., Jr.; Vreven, T.; Kudin, K. N.; Burant, J. C.; Millam, J. M.; Iyengar, S. S.; Tomasi, J.; Barone, V.; Mennucci, B.; Cossi, M.; Scalmani, G.; Rega, N.; Petersson, G. A.; Nakatsuji, H.; Hada, M.; Ehara, M.; Toyota, K.; Fukuda, R.; Hasegawa, J.; Ishida, M.; Nakajima, T.; Honda, Y.; Kitao, O.; Nakai, H.; Klene, M.; Li, X.; Knox, J. E.; Hratchian, H. P.; Cross, J. B.; Adamo, C.; Jaramillo, J.; Gomperts, R.; Stratmann, R. E.; Yazyev, O.; Austin, A. J.; Cammi, R.; Pomelli, C.; Ochterski, J. W.; Ayala, P. Y.; Morokuma, K.; Voth, G. A.; Salvador, P.; Dannenberg, J. J.; Zakrzewski, V. G.; Dapprich, S.; Daniels, A. D.; Strain, M. C.; Farkas, O.; Malick, D. K.; Rabuck, A. D.; Raghavachari, K.; Foresman, J. B.; Ortiz, J. V.; Cui, Q.; Baboul, A. G.; Clifford, S.; Cioslowski, J.; Stefanov, B. B.; Liu, G.; Liashenko, A.; Piskorz, P.; Komaromi, I.; Martin, R. L.; Fox, D. J.; Keith, T.; Al-Laham, M. A.; Peng, C. Y.; Nanayakkara, A.; Challacombe, M.; Gill, P. M. W.; Johnson, B.; Chen, W.; Wong, M. W.; Gonzalez, C.; Pople, J. A. *Gaussian 03*, Revision B.04; Gaussian, Inc.: Pittsburgh, PA, 2003.

(26) Jordan, K. D.; Wang, F. *Ann. Rev. Phys. Chem.* **2003**, *54*, 367.

(27) Hammer, N. I.; Diri, K.; Jordan, K. D.; Desfrançois, C.; Compton, R. N. *J. Chem. Phys.* **2003**, *119*, 3650.

(28) Hammer, N. I.; Hinde, R. J.; Compton, R. N.; Diri, K.; Jordan, K. D.; Radisic, D.; Stokes, S. T.; Bowen, K. H. *J. Chem. Phys.* **2004**, *120*, 685.

(29) Xu, S.; Nilles, J. M.; Bowen, K. H., Jr. *J. Chem. Phys.* **2003**, *119*, 10696.

(30) Serrallach, A.; Meyer, R.; Günthard, Hs. H. *J. Mol. Spectrosc.* **1974**, *52*, 94.

(31) Nelson, R. D.; Lide, D. R.; Maryott, A. A. Selected Values of Electric Dipole Moments for Molecules in the Gas Phase. *National Standard Reference Data Series-National Bureau of Standards 10*; NBS: Washington, DC, 1967.

(32) Chernyak, Y. *J. Chem. Eng. Data* **2006**, *51*, 416.